2018 International Symposium on Antennas and Propagation (ISAP 2018)
October 23~26, 2018 / Paradise Hotel Busan, Busan, Korea

Position Optimization of LF Array Antennas in a Small Device

Tae Heung Lim1, Jun Hur1, and Hosung Choo1
1 School of Electronic and Electrical Engineering Hongik University, Seoul, Korea

***Abstract* - In this paper, we analyzed the near magnetic field characteristics of LF antennas embedded in a small device. Array configuration with individual LF elements was optimized with the cost metric of the readable volume. At the optimized array position, a maximum readable volume of 8.36 m^3 is achieved, which is greater than the reference case with three LF antennas at the grid position of (1,6).**

***Index Terms* — LF antenna, Small device, Location optimization, Array configuration.**

1. Introduction

Due to the recent advances in wireless communications, internal vehicle systems are often handled with wireless devices without a direct connection. Small low frequency (LF) communication devices for vehicles usually perform unwired operations such as door opening and closing, engine control, and internal system management. The LF antenna in the small devices can maintain a wireless communication link with the vehicle system through a strong near magnetic field. This field strength is determined by the configuration of the LF antenna, such as the properties and dimensions of the ferrite core and the number of coil turns. In recent years, there has been a growing demand to embed LF antennas in small devices for integrating wireless communication system. Most of the LF coil antennas have been studied with EM properties in free space [1]-[3]. However, in-depth research on the field analysis as well as array configurations for LF antennas in small devices has not been carried out sufficiently.

In this paper, we investigate the near magnetic field characteristics of the LF antennas mounted on small devices. Based on the field analysis, we then optimize the positions for each LF array element within the device under test (DUT). To optimize the array configuration, we define the metric of the readable volume as the cost in the optimization process. Finally, the optimum position of each antenna in the small device is determined, and in this case, the near magnetic field strength is investigated in various ways.

2. Location optimization of LF array antenna

Fig. 1 presents the geometry of the LF antennas and the DUT with the dimensions of $w_2\times l_2\times h_2$ mm^3. Two types of the LF antenna are designed to generate magnetic fields along the *x*-, *y*-, and *z*-axis, respectively. To estimate the LF antenna performance, the ferrite cores (μ_r = 400, $tan\delta_\mu$ = 0.04) and coils are modeled as piecewise mesh triangles in FEKO EM simulation Software from Altair Engineering [4]. A low-profile cuboid type antenna generating the magnetic field dominantly along *x*- and *y*-axis is designed using the parameters l_1, w_1, and h_1 with a restricted height of h_2. The second type of the antenna has a cylindrical structure with a radius of *r*, so that the maximum magnetic flux density can be directed to the *z*-axis. Each ferrite core is wound by the wires with the same number of turns N_x, N_y, and N_z. The DUT with all six sides of perfect electric conductor (PEC) is considered in this study to mount the LF antennas. The detailed design parameters are listed as follows:
l_1 = 11.4 mm, w_1 = 3.55 mm, h_1 = 2.35 mm, l_2 = 161.4 mm, w_2 = 68.8 mm, h_2 =7.9 mm, and N_x, N_y, N_z = 200.

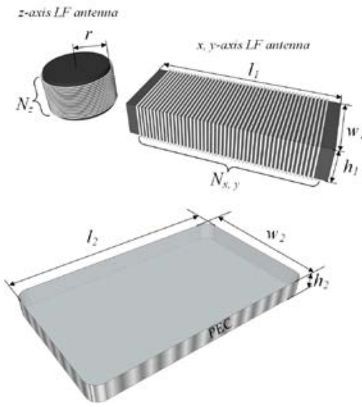

Fig. 1. Geometry of the LF antennas with the DUT.

Fig. 2 illustrates the possible locations with the grid in the small device for positioning each antenna in the optimization process. The location parameters dx_n and dy_n are along *x*- and *y*-axis with an antenna index (*n* = 1, 2, and 3).

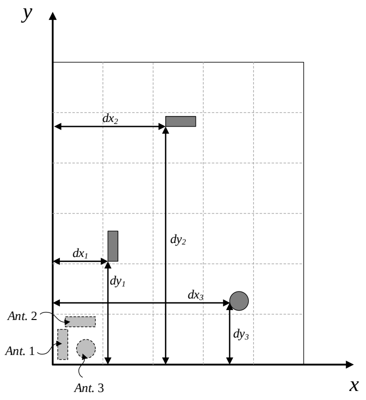

Fig. 2. Conceptual position optimization for each LF antenna.

Near field distributions are quantized by 201×201 points in *xy*-plane and by 21 layers along the *z*-axis (−1 m ≤ *x* ≤ 1 m, −1 m ≤ *y* ≤ 1 m, and −1 m ≤ *z* ≤ 1 m). We calculate the Poynting vector values at each point to estimate the readable area in *xy*-plane above a threshold value of −95 dBm. These areas are equally spaced along the *z*-axis with an interval of 0.05 m and then summed to make the total volume that indicates the overall readable volume:

$$\text{Readable volume} = \sum_{k=1}^{N_h} A_k \Delta h. \qquad (1)$$

N_h is the maximum number of layers, and A_k is the area of each layer over the threshold value. Δh is the equal interval of each layer. Fig. 3 shows the readable volumes of the LF array when three LF elements are integrated and moving in the grid. The maximum value of 7.4 m^3 is obtained at the grid point of (1,6).

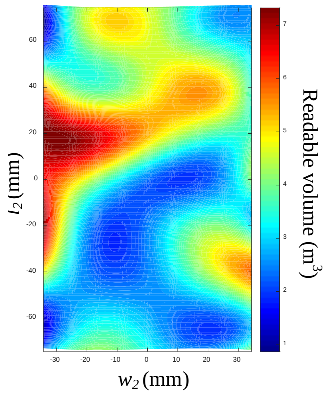

Fig. 3. Readable volume according to the location of the three integrated LF antennas.

We then optimize three antenna positions separately in the grid. In this optimization, the best solution that maximize the readable volume, is found among the total of 46,656 searching space. The readable areas according to the height are presented in Fig. 4, and the optimized positions of the LF antennas in the small device (dx_1 = 1.2 mm dx_2 = 19.2 mm, dx_3 = 10.6 mm, dy_1 = 80.8 mm, dy_2 = 45.6 mm, and dy_3 = 86.1 mm) is represented in the inset figure. The maximum readable area is 3.42 m^2 at the height of 0 m, and the readable volume is 8.36 m^3. The result shows that the position optimization of each LF antenna can increase the readable volume effectively compared to that of the three integrated LF antennas.

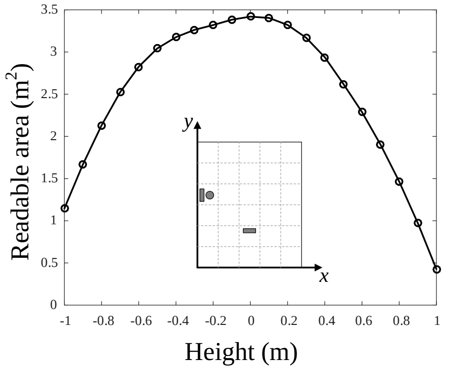

Fig. 4. Readable area of the optimal array configuration.

3. Conclusion

We analyzed the near magnetic field characteristics of LF antennas embedded in a small device. Based on the field analysis, the positions for three LF elements are optimized to achieve the maximum readable volume. The optimized array configuration provided a readable volume of 8.36 m^3 that is greater than the integrated three LF antennas.

References

[1] F. Paredes, I. Cairo, S. Zuffanelli, G. Zamora, J. Bonache, and F. Martin, "Compact design of UHF RFID and NFC antennas for mobile phones," *IET Microw., Antennas Propag.*, vol. 11, no. 7, pp. 1016-1019, Jan. 2018.

[2] S. T. G. Maguire and P. A. Robertson, "Low frequency radio polarization sensor with applications in attitude estimation," *IEEE Sens. J.*, vol. 15, no. 12, pp. 7304-7311, Dec. 2015.

[3] A. Kiourti and K. S. Nikita, "Implantable antennas: a tutorial on design, fabrication, and in Vitro/in Vivo testing," *IEEE Microw. Mag.*, vol. 15, no. 4, pp. 77-91, Jun. 2014.

[4] FEKO EM Simulation Software, Altair Engineering Inc., 2018. Available: http://www.altair.co.kr.